Organic Geochemistry 115 (2018) 46–56

Contents lists available at ScienceDirect

Organic Geochemistry

journal homepage: www.elsevier.com/locate/orggeochem

A rapid and precise method for the analysis of underivatized amino acids in natural samples using volatile-ion-pairing reverse-phase liquid chromatography–electrospray ionization tandem mass spectrometry

Jack A. Hutchings [a,*], Michael R. Shields [a], Thomas S. Bianchi [a], Edward A.G. Schuur [b]

[a] Department of Geological Sciences, University of Florida, 241 Williamson Hall, Gainesville, FL 32611, USA
[b] Department of Biological Sciences (Box 5640), Northern Arizona University, Flagstaff, AZ 86011, USA

ARTICLE INFO

Article history:
Received 21 April 2017
Received in revised form 16 October 2017
Accepted 20 October 2017
Available online 14 November 2017

ABSTRACT

Amino acids are effective tracers of organic carbon and nitrogen cycling in natural substrates. However, total analytical time can be long due to extraction, derivatization, and chromatography. Here, we present a liquid chromatographic separation of 19 naturally occurring amino acids requiring no derivatization using triple-quadrupole mass spectrometry. This method builds on recent advances in volatile ion pairing and was applied to natural soil samples collected from two distinct systems with highly variable organic C contents. Separation and quantification of amino acids were achieved with an 18 min sample-to-sample run time employing a one-point standard addition to account for variable matrix effects during ionization. Detection limits ranged from 5.9 to 187.5 fmol (mean 30.0 fmol) while instrumental precision averaged 5.8% and 12.0% for intra- and inter-day error, respectively. The highest yields (mean > 100 μmol/g C) in our natural substrates were observed for glycine, aspartic acid, alanine, and glutamic acid while low yields (mean < 20 μmol/g C) were observed for all non-proteinogenic amino acids as well as histidine and tyrosine. A typical hot acid hydrolysis in 6N HCl was used and hydrolyzates were diluted and filtered rather than being subjected to solid-phase extraction or similar techniques, which require significant investment of time during sample preparation. This method enables high throughput and reliable analysis of hydrolyzable amino acids, while also reducing user workload and instrument time compared to previous techniques. The Alaskan tundra system had significantly higher absolute yields of amino acids (mean 88.4 vs 25.6 μmol/g dry sediment), in part driven by higher organic C concentrations, while the Louisiana delta system had significantly higher organic C normalized yields of amino acids (mean 1492.5 vs 541.6 μmol/g C). Despite these differences, both systems exhibited broadly similar mole-percent amino acid compositions.

1. Introduction

Amino acids are the fundamental building blocks of proteins and, thus, are among the most ubiquitous biological compounds found on Earth. The amino acid composition of complex, natural substrates has been used to investigate a number of biogeochemical processes in both aquatic and terrestrial settings, including organic matter sources (West et al., 1987; Van Hees et al., 2005; Duan and Bianchi, 2007; Hobara et al., 2014) and degradation state (Dauwe et al., 1999; Menzel et al., 2015; Philben et al., 2016). There exists many secondary amino acids such as hydroxyproline (Philben and Benner, 2013; Philben et al., 2016) and gamma-aminobutyric acid (Cowie and Hedges, 1994; Dauwe and Middelburg, 1998) that are indicative of specific sources and processes. Amino acids often constitute a significant fraction of nitrogen in soils (Friedel and Scheller, 2002) and thus their form and turnover rates can influence nutrient availability for primary producers (Tremblay and Benner, 2006; Farrell et al., 2013). In marine settings, proteinogenic amino acids have also been used as biomarkers for organic nitrogen and show good potential for use as proxies for intact protein sequences in both the water column and in sediments (Moore et al., 2014a, 2014b). Adapting methodologies that allow rapid analysis of amino acids in complex, geological matrices has significant potential for furthering our understanding of the composition and fate of organic matter in natural systems.

Commonly employed methods (Table 1) of analyzing amino acids require chemical transformation (i.e., derivatization) prior to fluorescent or colorimetric detection using *o*-phthaldialdehyde (Lindroth and Mopper, 1979; Jarret et al., 1986), ninhydrin

* Corresponding author.
E-mail addresses: jahutch2@gmail.com, jahutch2@ufl.edu (J.A. Hutchings).

https://doi.org/10.1016/j.orggeochem.2017.10.007
0146-6380/

Table 1
Common amino acid methods applied to soils.

Separation	Detection	Analytical preparation	Analysis time (min)	Amino acids analyzed (#)	Mean LOD (fmol)	References
LC	UV	Derivatization with o-phthaldialdehyde, 2-mercaptoethanol, and polyoxyethylene lauryl ether	35[+]	18	50–500	Jarret et al. (1986) and Werdin-Pfisterer et al. (2009)
GC	Flame Ionization or MS	De-salting by cation exchange resin; derivatization with isopropanol and pentafluoropropionic anhydride	31.25	15 (28 including enantiomers)	521[*]	Amelung and Zhang (2001)
GC	Flame Ionization	Purification by cation exchange resin; derivatization with propyl chloroformate	11.5[+]	13	Not Reported	Kugler et al. (2006) and Roberts and Jones (2008)
LC	MS–MS	De-salting by cation exchange resin	26[+]	20	719	Liu et al. (2008)
LC	MS	De-salting by cation exchange resin; derivatization with 6-aminoquinolyl-N-hydroxysuccinimidyl carbamate	50	17	3829	Hou et al. (2009)
LC	MS–MS	Desalting by cation exchange resin	23	20	667	Gao et al. (2016)
LC	MS–MS	Dilution of hydrolyzate to ~pH 1 using H_2O	18 (2 × 9 min)	19	30	Present Study

[+] Inter-sample equilibration or injection time not specified.
[*] Converted from the reported injection mass using an average value of 128 g/mol for analyzed amino acids.

(Rosen, 1957), or other agents (Udenfriend et al., 1972). These methods also tend to have long analytical times (Lindroth and Mopper, 1979) that limit either sample throughput or robust quantitation of error. Recently, the usage of mass spectrometers coupled to chromatographic schemes has been used to detect amino acids both with (Hou et al., 2009; Kaspar et al., 2009; Harder et al., 2011) and without (Petritis et al., 1999; Piraud et al., 2005; Liu et al., 2008) derivatization. The simplicity of underivatized analysis is attractive for reasons such as preparation time and cost, although poor ionization and fragmentation efficiencies of certain amino acids such as glycine and alanine may result in unattractive limits of detection in some settings, though ion source mechanism and configuration can influence relative efficiencies (Petritis et al., 2000, 2002; de Person et al., 2008). Perfluorinated carboxylic acids have been successfully used as ion-pairing agents to enable the retention of more polar amino acids while still being volatile enough to be suitable for mass spectrometry (Petritis et al., 1999, 2000; Piraud et al., 2005). However, there are conflicting reports of whether using perfluorinated carboxylic acids enhance (de Person et al., 2008) or suppress (Apffel et al., 1995; Piraud et al., 2005) the ionization of amino acids.

The ability of triple-quadrupole mass spectrometry to decrease background signal is critical to many modern analyses. However, this scan mode prevents the detection of co-eluting compounds in the sample matrix that, due to enhancement or suppression of ionization, can affect the signal of the analyte (Matuszewski et al., 2003; Huang et al., 2012). It is well recognized that matrix effects can influence ion sources commonly coupled to liquid chromatographs, including electrospray and atmospheric pressure chemical ion sources. Typically, different regions of a chromatogram are affected by matrix effects, which can be accounted for with the use of internal recovery standards. When choosing internal standards, it is often recommended that the standard be as close in composition to the analyte as possible. A costly but highly effective strategy is to use isotopologues of the target analytes that have their total mass shifted sufficiently far away from the native analyte (typically at least 5 Da). An equally effective but more laborious strategy is that of standard addition, where a sample is measured with and without the addition of a known mass of each analyte, allowing for the accurate determination of analyte mass – even in the presence of a strong matrix effect. Traditional standard addition schemes include multiple levels of internal standard spikes resulting in a sample-specific calibration curve. However, recent work demonstrated that a single level of addition can accurately determine analyte mass without any significant loss of precision (Ellison and Thompson, 2008).

The overall goal of this work was to apply the analysis of underivatized amino acids to natural soil and sediment samples using a perfluorinated carboxylic acid as a volatile ion-pairing agent on a high-pressure liquid chromatograph coupled to a heated electrospray ion source and a triple-quadrupole mass spectrometer. This analytical approach is well-developed in the recent literature (Petritis et al., 1999, 2000, 2002; Piraud et al., 2005; Liu et al., 2008; Waterval et al., 2009; Konn et al., 2015) with applications to a wide range of sample matrices, many of which require correction for ion-source matrix effects. The mineral and organic content of environmental samples often results in an exceptionally complex matrix that can affect both the chromatography and ionization efficiency on a per-sample basis. Here, we managed this by testing chromatographic conditions against a range of samples and by performing on-line standard addition for quantification. Our objectives specifically targeted hydrolyzable amino acids, however this analytical method is also appropriate for measuring free amino acids, given appropriate concentrations or sample preparation (Liu et al., 2008). To the best of our knowledge, this is the first method documenting the use of perfluorinated carboxylic acids as ion-pairing agents for the analysis of natural soil and sediment amino acid hydrolyzates.

2. Methods and materials

2.1. Standards and chemicals

A mixture (Table 2) of 17 amino acids (Pierce Amino Acid Standard H, Thermo Scientific #20088) as well as trans-4-hydroxy-L-proline (Sigma Aldrich #H54409), gamma-aminobutyric acid (Sigma Aldrich #03835), muramic acid (Sigma Aldrich #M2503), and 2,6-diaminopimelic acid (Sigma Aldrich #D1377) were used as standards. Nonafluoropentanoic acid (NFPA, Sigma Aldrich #396575) was used as the ion-pairing agent for retention of polar amino acids during liquid chromatography. LCMS-grade acetonitrile (ACN, Fisher #A955) and methanol (MeOH, Fisher #A456) were used for elution of amino acids during liquid chromatographic separation and for post-run flushing, respectively. Concentrated HCl (Fisher #A144) was used to make solutions of concentrations indicated below and all aqueous solutions were prepared using deionized water further purified on a Nanopure water purification system to a resistivity of 18.2 MΩ cm. Ammonium hydroxide (NH_4OH, Fisher #A669), Dowex 50WX8 200–400 mesh resin (Fisher #AC335351000), and oxalic acid (Sigma Aldrich #247537) were used during sample clean-up. LCMS-grade

Table 2
Analytical settings and precision metrics.

Name	Code	RT (min)	Precursor (*m*/*z*)	Product (*m*/*z*)	Collision energy (V)	LOD (fmol)
Hydroxyproline	Hyp	0.21	132.1	86.2	13.0	12.4
Serine	Ser	0.22	106.2	60.3	10.3	23.4
Glycine	Gly	0.23	76.2	30.6	10.3	187.5
Aspartic acid	Asp	0.23	134.1	88.2	10.3	23.4
Threonine	Thr	0.26	120.2	102.2	8.0	93.8
Glutamic acid	Glu	0.26	148.1	84.2	14.2	11.7
Alanine	Ala	0.29	90.2	44.4	6.0	46.9
Proline	Pro	0.31	116.2	70.3	13.1	23.4
Gamma-aminobutyric acid	GABA	0.35	104.2	87.2	10.3	15.9
Muramic acid	MurA	0.40	252.3	234.0	10.3	31.3
Valine	Val	0.64	118.2	72.3	10.3	11.7
Diaminopimelic acid	DAPA	0.81	191.1	128.1	14.1	6.3
Tyrosine	Tyr	0.93	182.0	165.0	10.3	11.7
Histidine	His	1.11	156.1	110.1	12.0	23.4
Lysine	Lys	1.44	147.2	84.2	15.9	11.7
Isoleucine	Ile	1.55	132.2	86.2	10.3	11.7
Leucine	Leu	1.85	132.2	86.2	10.3	11.7
Arginine	Arg	2.05	175.1	70.3	22.0	5.9
Phenylalanine	Phe	2.70	166.1	120.1	10.3	5.9

isopropanol (Fisher #A461) was used during auto-sampler needle rinsing. All glassware was baked at 450 °C for 4 h in a muffle furnace prior to use.

2.2. Sample collection and treatment

A permafrost soil core was collected in March 2015 using a UKB-12/25 drilling rig from the Eight Mile Lake watershed outside Healy, Alaska (63°52′44.0″N, 149°15′10.4″W). The local ecosystem is a moist acidic tundra dominated by the tussock-forming sedge, *Eriophorum vaginatum*. The site has an organic-rich topsoil underlain by glacially sourced loess and till (Trucco et al., 2012), which results in subsamples from this core representing a wide range of OC and mineral contents (Table 3). All collected samples were processed in a cold room at the University of Alaska Fairbanks, shipped frozen to the University of Florida, and kept frozen at −20 °C until being subsampled for this experiment.

For comparison, we included subsamples from a series of coastal sediment cores extracted from the Wax Lake delta, Louisiana (29°30′25″N 91°27′36″W) during a field campaign in 2015. The Wax Lake delta is sand-dominated, actively prograding, and exhibits a range of subaerial colonization by plants (Shields et al., 2016). Immediately following collection, samples were transported to the University of Florida, kept in a cold room at 4 °C prior to processing and sub-sectioning, and sub-sections were kept frozen until final preparation.

In addition to field samples, two National Institute of Standards and Technology standard reference materials were included for analysis: SRM 1944, New Jersey waterway sediment, and SRM 1547, peach leaves.

2.3. Sample preparation and hydrolysis

Frozen samples were freeze-dried and ground to homogeneity using a Spex 8000 M Mixer/Mill prior to analysis. Total carbon (TC) and nitrogen (TN) contents were determined using a Carlo Erba NA 1500 elemental analyzer. Total inorganic carbon (TIC) contents were determined by measuring carbon dioxide gas produced after acidification with phosphoric acid. TOC was defined as the difference between TC and TIC.

An amount of sample equivalent to 3 ± 1 mg organic carbon was added to 20 mL screw-cap test tubes and 1 mL of 6 N HCl was added to each test tube. The oxygen content of the headspace in each tube was minimized using an N_2 blowdown station, whereby an active nozzle was inserted into the tube and capped with PTFE-lined caps, while under the N_2 stream of 4 adjacent nozzles. Tubes were then placed in a muffle furnace at 110 °C for 20 h. After hydrolysis, tubes were allowed to cool before adding 5 mL H_2O to each, which brought each sample to a concentration of approximately 1 N HCl. Aliquots of hydrolyzates (0.15 mL) were then further diluted ten-fold (using H_2O) to a final concentration of approximately 0.1 N HCl and a total volume of 1.5 mL.

Table 3
Sample information.

Source	Sample ID	Core depth (cm)	TOC (%)	TN (%)	Bulk density (g/cm^3)	Replicate extractions	Extraction precision (RSD%)	THAA (μmol/g dry sediment)	Mean matrix effect (%)
NIST	SRM_1547	–	44.65	2.94	–	6	12.9	1123.9	93.0
NIST	SRM_1944	–	4.40	–	–	6	13.1	60.3	81.5
Eight Mile Lake	EML_020	20	43.29	1.27	0.07	2	10.1	241.6	98.9
Eight Mile Lake	EML_060	60	29.55	1.14	0.31	2	8	159.3	97.4
Eight Mile Lake	EML_101	101	4.49	0.29	0.35	2	13	28.7	95.1
Eight Mile Lake	EML_141	141	0.79	ND	1.15	2	28.7	2.3	88.8
Eight Mile Lake	EML_183	183	1.47	0.08	0.51	2	16.2	10.0	87.4
Wax Lake Delta	WLD_1-02	2	2.33	0.21	0.76	2	22.1	59.5	80.0
Wax Lake Delta	WLD_1-40	40	1.18	0.09	1.30	2	11.5	21.9	81.9
Wax Lake Delta	WLD_1-80	80	0.17	ND	2.00	2	30.3	0.6	86.4
Wax Lake Delta	WLD_4-06	6	2.31	0.17	1.04	2	39.1	42.7	91.5
Wax Lake Delta	WLD_4-40	40	0.40	0.03	1.82	2	19.6	3.4	75.0

ND indicates below detection limit.
Dash indicates not measured or available.

Hydrolyzates were then filtered using 0.2 μm nylon membrane syringe filters (Scientific Equipment of Houston, #NY013022-100) into 1.5 mL auto-sampler vials for analysis.

A subset of samples was subjected to post-hydrolysis, solid phase extraction clean-up to remove salts and concentrate amino acids following literature protocols (Amelung and Zhang, 2001; Liu et al., 2008). Columns constructed from glass Pasteur pipettes (~2 mL total volume) plugged with glass wool were gravity packed with ~1.5 mL of a slurry of Dowex strong cation exchange resin in H_2O. After settling, approximately 1.5 mL of headspace remained in each column. Columns were primed by sequentially loading 4.5 mL 2 N NH_4OH, 4.5 mL 2 N HCl, and 4.5 mL H_2O. Once primed, hydrolyzates were spiked with an internal recovery standard (75 μL of 2 mM norvaline in 0.1 N HCl), diluted to approximately 1 N HCl using H_2O, and then loaded onto the columns. Columns were sequentially rinsed with 3 mL 0.1 M oxalic acid adjusted to pH 1.6–1.8 with NH_4OH, 3 mL 0.01 N HCl, and 3 mL H_2O. After rinsing, clean 20 mL scintillation vials were placed under each column and samples were eluted using 7.5 mL of 2 N NH_4OH. Eluted samples were placed on an N_2 dry-down station, heated to 50 °C, and blown-down for 20 min to reduce the concentration of NH_4OH via de-gassing as NH_3. Vials were then capped, frozen, freeze-dried, re-dissolved in 1.5 mL 0.1 N HCl, and filtered using 0.2 μm nylon membrane syringe filters (Scientific Equipment of Houston, # NY013022-100) into 1.5 mL vials for analysis.

2.4. Instrumentation

Amino acids were analyzed by ultra-high-performance liquid chromatography (LC) coupled to a heated electrospray ion source (H-ESI) that fed directly into a triple-quadrupole mass spectrometer (MS–MS). LC was performed by a Dionex Ultimate 3000 system using on-line solvent degassing and auto-sampler temperature control (5 °C). A Thermo Scientific TSQ Endura was used for H-ESI and MS–MS.

Separation (Fig. 1) was achieved on a javelin-style Hypersil Gold aQ C18 reversed-phase column (20 × 2.1 mm I.D., particle size 1.9 μm; Unity Lab Services #00109-01-00013) without a guard column, but fitted with a pre-column filter (Thermofisher #88200). An isocratic elution scheme was used with the mobile phase consisting of 10 mM NFPA in H_2O with 8% by volume ACN and a total duration of 3.5 min. After 3.5 min of elution, flow was switched to 100% MeOH for 2.5 min to flush the column and ion source of any remaining ion-pairing agent. The flow rate was 500 μL/min and a total injection volume of 3 μL was used for all experiments. Analytical blanks of 0.1 N HCl and mixed standard injections were used at the start, end, and every four samples of each batch of 10–20 samples. A clean-up method of 100% methanol at 200 μL/min for 20 min was used with the first 5 min directed to waste (allowing for equilibration) and the remainder to the H-ESI, set at the manufacturer's recommendations to further clean the ion source between batches. Post-column dead volume was minimized to ~8 μL by interfacing our 'javelin' column's male end directly into the pre-mass spectrometer Rheodyne divert valve, which diverted to waste during the standard addition procedure (see below) and from 0 to 0.1 min during analysis.

Samples were injected according to a one-point standard addition scheme performed via a 'user defined program' on the auto-sampler with additions of a 40 μM mixed standard that contained all amino acids used in this study (Table 2). All needle washes were performed on-line using 100 μL of isopropanol. For each injection, the auto-sampler needle was washed, a 1 μL pocket of air was drawn into the sample loop, 1.5 μL of either a blank (0.1 N HCl) or the mixed standard was drawn into the sample loop, the needle washed, 1.5 μL of sample was drawn into the sample loop, and the needle was then washed a final time before injection; this also served as a delay period to allow better mixing of the sample loop contents. During the analytical run, the needle-wash reservoir was filled in preparation for the next sample. The sample preparation process required ~3 min and, combined with the HPLC run-time of 6 min, resulted in a total injection-to-injection runtime of ~9 min. Each sample experienced two injections to accommodate both blank and standard additions resulting in a sample-to-sample runtime of ~18 min. Blank injections consisted of 3 μL of 0.1 N HCl, and mixed standard injections consisted of 1.5 μL mixed standard and 1.5 μL of blank to keep the injection volume consistent with sample injections.

Ion source and mass spectrometer settings were optimized first by direct syringe injection of the manufacturer's tuning solution of polytyrosine (Fisher Scientific #00301-22925) and then by flow syringe injection of a mixture of 40 μM in 0.1 M HCl of each amino acid used here (Table 2) into a 495 μL/min flow of the analytical mobile phase described above. All syringe injections were set to 5 μL/min to achieve a total flow rate of 500 μL/min. Optimized H-ESI parameters were an electrospray voltage of 4000 V, a sheath gas (primary nebulizing agent) of 32.5 arbitrary units, a heated auxiliary gas (assisting nebulizing agent) of 10 arbitrary units, a vaporizer temperature of 200 °C and an ion-transfer tube temperature of 300 °C. Nitrogen (99.998% purity, AirGas) was used for all H-ESI gas flows while Argon (99.999% purity, AirGas) was used at 1.5 mTorr in the collision cell. MS–MS transitions were determined by syringe infusion of solutions containing individual amino acids using the same infusion scheme as above and the top 3 product ions were identified using the manufacturer automated MS–MS optimization program. During analysis, the highest signal MS–MS transition was used for each analyte and timing was based on the retention time of the analyte, with a cycle time of 1000 ms and Q1 and Q3 mass resolutions both set to 0.7 full width at half maximum. This approach resulted in a minimum dwell time of ~83 ms.

2.5. Quantitative approach

The one-point standard injection approach of Ellison and Thompson (2008) was applied using two or four injections per sample to either model or directly calculate instrumental precision, respectively. The sample injection mass (M_{Raw}) was quantified using the following equation:

$$M_{Raw} = (R_{Raw} \times M_{Add})/(R_{Add} - R_{Raw}) \quad (1)$$

where M_{Add} is the mass of standard injected in a spiked sample, R_{Raw} is the average instrument response of the unspiked sample, and R_{Add} is the average instrument response of the sample spiked with the mixed standard. Intra-day instrumental error was assessed using two strategies. A calculated intra-day relative standard deviation (RSD) was based on a total of four sample injections (two each of blank and standard additions), expressed as a percentage, and calculated using the equation:

$$RSD(M_{Raw}) = \frac{1}{R_{Raw} \times (R_{Add} - R_{Raw})} \times (var_{Raw} \times R_{Add}^2 + var_{Add} \times R_{Raw}^2)^{1/2} \times 100 \quad (2)$$

where var_{Raw} and var_{Add} are the variances of the unspiked and spiked sample injection responses, respectively. A simulated intra-day RSD was determined by generating normal distributions of sample areas using the RSDs of standard injections that bracketed every other sample in a batch. These distributions were then re-sampled using a balanced bootstrap approach to generate intra-day RSD.

Calculation of a matrix effect (ME) used the following equation:

$$ME = R_{Add}/(R_{Std} + R_{Raw}) \quad (3)$$

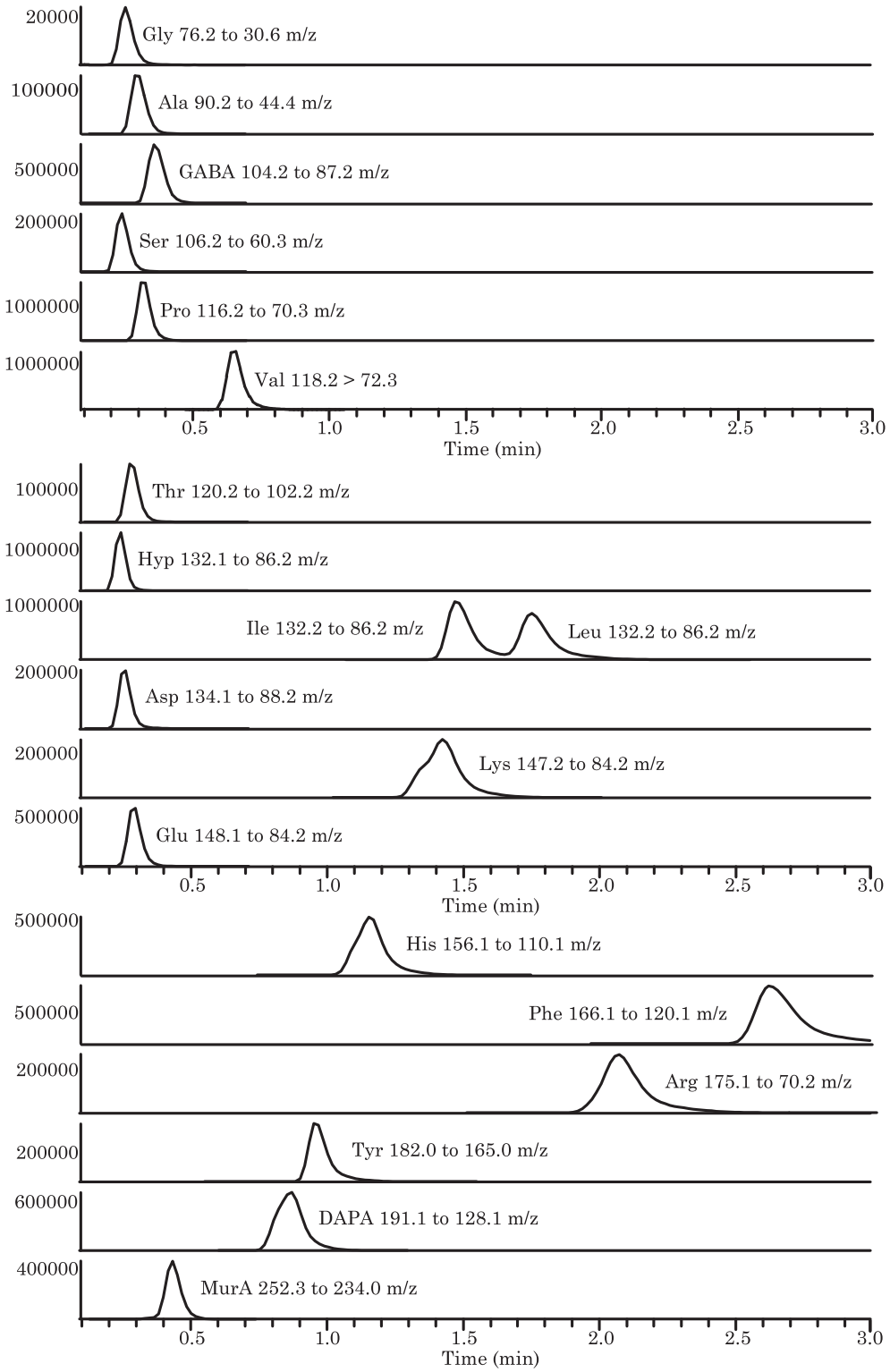

Fig. 1. A typical extracted ion chromatogram showing mass transitions for each analyte. The Y-axis is instrument response in arbitrary units. See Table 2 for analyte abbreviations.

where R_{Std} is the average instrument response of mixed-standard injections within a batch of 10–20 samples. Using this metric, ME > 1 indicated signal enhancement and ME < 1 indicated signal suppression. Typically, a matrix effect of less than ~5% is considered negligible. Prior to quantification, all injections were blank subtracted accounting for sample-specific matrix effect and blank addition using the following equation:

$$R_{Sub} = R_{Unsub} - R_{Blank} \times ME \times f_{Blank} \quad (4)$$

where R_{Sub} is the blank subtracted response, R_{Unsub} is the unsubtracted response, R_{Blank} is the average response of blank injections within a sample batch, and f_{Blank} is the fraction of the injection composed of blank 'balance', equal to 0.5 corresponding to 1.5 μL of blank in a 3 μL injection.

Initial peak processing and export was performed using the Thermofisher XCalibur 2.0 software. Exported data was briefly reformatted into a processing template using Microsoft Excel and then imported to the statistical computing software R (R Core Team, 2017) for quantification. An example data set and processing script can be found in the online supplement. Statistical significance was assessed using 95% confidence intervals generated using a balanced bootstrap approach (Davison et al., 1986).

3. Results and discussion

3.1. Chromatographic optimization

The use of MS–MS obviated the need for complete separation (Fig. 1) of analytes with the exception of isobars with identical mass transitions. Separation of Hyp from Ile/Leu was trivial given the large difference in retention time (RT), while optimizing the Ile/Leu separation was the focus of chromatographic development. A primary use of NFPA is the retention of amino acids that would otherwise not be retained. Here, these include all amino acids with RTs between 0.22 and 0.31 min. While we initially attempted to follow gradient separation schemes found in the literature (Petritis et al., 2000; Piraud et al., 2003; Liu et al., 2008; Konn et al., 2015), brief testing with isocratic elution yielded promising results that were then refined by testing a range of NFPA concentrations (1, 5, 10, and 20 mM) and a range of ACN volume contributions (0–20% v/v in steps of 2%), with the latter accomplished using dual pumps during development and pre-mixing during validation. During this phase, the post-analysis flush of the column was accomplished with 100% ACN. During initial method development, the high end of the NFPA range (20 mM) was chosen to enable maximum retention while not erring towards potential ion suppression issues (de Person et al., 2008). This concentration of NFPA resulted in a trend of decreasing instrument signal within a sample batch that tended to reach as low as 50% of the initial signal intensity at the start of a batch. As the post-batch, end-of-day ion source cleaning used 100% MeOH and returned the instrument response to the levels experienced before a batch, we tested and implemented two strategies to eliminate this problem: a lower NFPA concentration of 10 mM and the use of MeOH as the post-analysis organic solvent. This approach eliminated obvious signal drift within a sample batch and resulted in mixed-standard injections that bracketed every other sample in a batch to have an average RSD of 3.8 ± 0.5% (mean ± SD). The use of MeOH at the end of each injection may also assist in preventing long-term NFPA-related issues of retention time shifts experienced elsewhere (Qu et al., 2002; Piraud et al., 2005; Liu et al., 2008), but we have not experienced this issue and thus cannot confirm this.

Minimizing our post-column dead volume was critical to acceptable separation of Ile/Leu due to post-column analyte diffusion, and while our 'javelin' column design is uncommon (female-in fitting and male-out fitting), a larger, but likely acceptable, dead volume should be achievable using short, small-volume tubing from a normal analytical column (e.g., Fisher # 25302-022130) to the MS divert valve. This strategy prevented the use of a column oven for precise temperature control, but our laboratory space is maintained between 21–25 °C and this temperature variation had no noticeable effect on retention time.

The combined effects of partial separation and MS–MS is still susceptible to matrix effects (discussed later) and the relatively rare co-elution of an unwanted compound with a similar mass transition to an analyte of interest. To assess this, a small subset of samples was analyzed, scanning for the top three (by signal) mass transitions of each compound to detect whether any additional peaks appear under specific transitions. The only significant co-elution of an isobar with at least one identical mass transition occurred with serine and a natural product tentatively identified as diethanolamine using a NIST MS–MS library. The interfering compound shared two of the top three transitions with serine, but use of the second highest transition eliminated this interference. Final quantification and routine analysis of all samples used the single mass transition from each analyte shown in Table 2.

3.2. Calibration

A 250 μM standard mixture of the 20 amino acids used here was prepared and serially diluted 17 times using 50% steps to a concentration of ~950 pM to determine the limits of detection and of linear response. The dilution series was serially injected three times to account for any signal drift and 3 μL injections were used. The linear range spanned from the limit of detection for each amino acid to an injection amount of ~100 pmol. No attempt was made to determine the upper end of the dynamic range nor to determine an appropriate regression for the dynamic range. The sample standard addition scheme and the concentration of the operating mixed standard (40 μM) allowed for injections to approach, but not exceed, the observed linear range.

3.3. Sample preparation

Two post-hydrolysis sample handling procedures were tested: dilution of hydrolyzate to ~0.1 N HCl and SPE clean-up. Development of the method initially followed the common literature usage of a strong cation exchange resin (Table 1). However, we found that SPE de-salted samples still exhibited instrument matrix effects, had high but variable recovery (mean of 96.4% and RSD of 42.2%), and had replicate extractions that exhibited poor precision (mean RSD of 44.4%). However, the observed amino acid concentrations of SPE samples indicated the possibility of simply diluting hydrolyzates to minimize the effect of salts in hydrolyzates. Using this strategy, extraction precision was improved (Table 3, mean RSD of 18.7%) and the lengthy sample handling time associated with execution of SPE was eliminated. Hydrolyzate dilution was adopted for all sample analyses presented here and has had no ill effects on the ion source over the more than 500 injections made during development and initial usage of this method by our laboratory. Over the same period, no loss of performance or peak shape was observed during chromatographic separation despite our sample injection pH of ~1 being outside the manufacturer's stable pH range of 2–9 for this packing media.

The amino acids cystine and methionine had consistently low concentrations in hydrolyzates and are excluded here. The loss of these compounds during hot HCl hydrolysis is well-described in the literature and various alternative approaches exist if quantification of these is necessary (Fountoulakis and Lahm, 1998).

3.4. Matrix effects

The complex organic and mineral matrix of natural samples combined with ESI source technology lead to the expectation of ionization effects. Average analyte matrix effects organized by retention time (Fig. 2) revealed early signal suppression between 0.2–0.3 min and large suppression around 2 min. As our dilution strategy does not remove salts and other compounds found in soils and sediments, we expected to experience some degree of matrix suppression early in the chromatograms for low carbon (i.e., high mineral) samples. This is supported by analysis of the data, which shows that samples with < 2% TOC had, averaged by analyte, 7% greater matrix suppression than samples > 2% TOC ($p < 0.05$, paired bootstrap). Organic carbon content differences between the two sites also exhibited this effect, with WLD (mean 1.3% TOC) showing

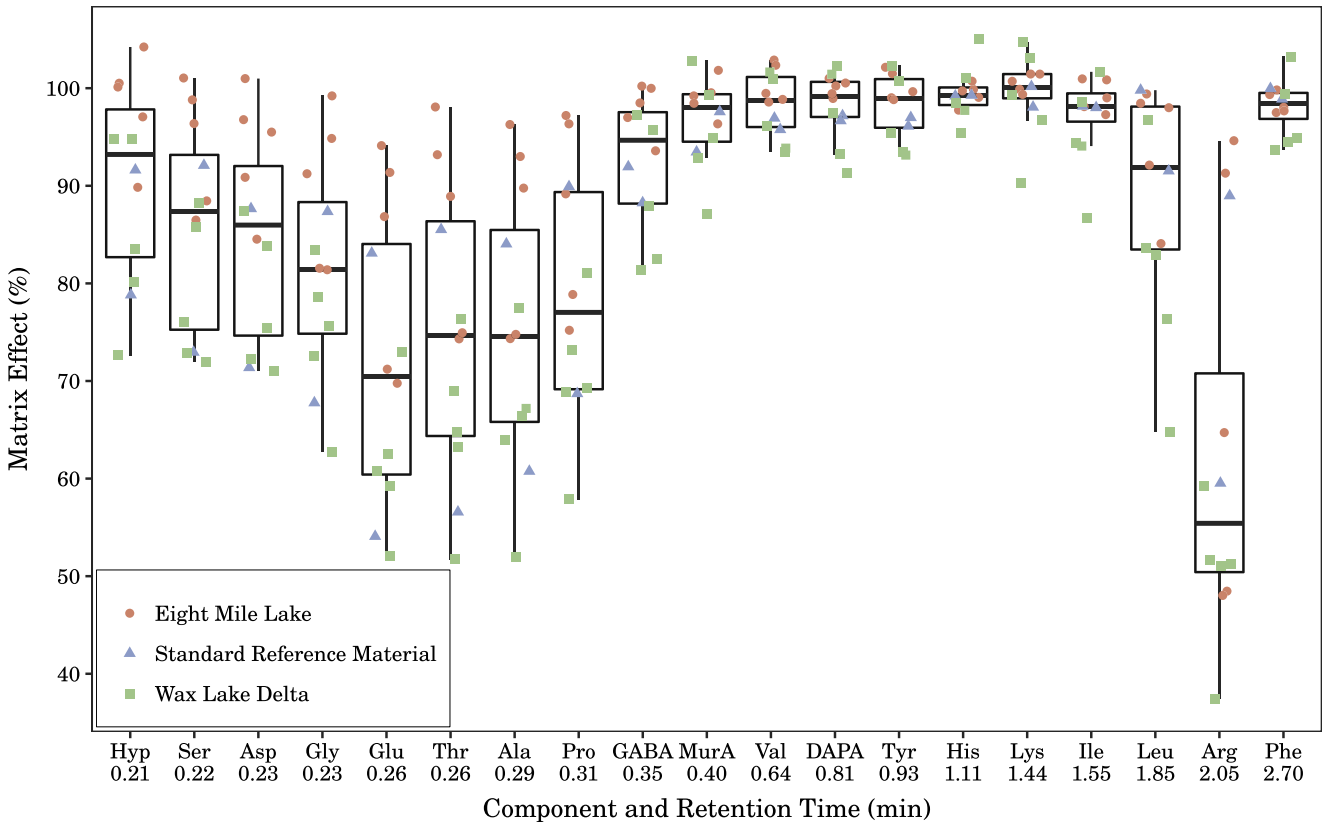

Fig. 2. Boxplots of matrix effects for each analyte, sorted by retention time. Note that the X-axis uses ordinal and not interval spacing.

a 10.5% greater matrix suppression ($p < 0.05$, paired bootstrap) than EML (mean 15.9% TOC). Samples at greater depths tended to have lower TOC values (Table 3), but depth only significantly predicted a sample's mean matrix effect at EML ($r^2 = 0.94$, $p < 0.05$). SRM 1547, composed of homogenized peach leaves, still showed a range of matrix effects with as much as ~17% suppression for early eluting analytes, indicating that some degree of interference comes from the organic matrix of a sample. The highly variable matrix effects on a per-analyte basis shown in Fig. 2 highlights the need for a full standard addition scheme to properly quantify these samples.

3.5. Analytical precision

Analytical precision was assessed across three scales: intra-day, inter-day, and procedural precision. Intra-day precision was calculated both by error propagation of duplicate injections of blank- and standard-added samples, as well as by simulation of sample injection precision using mixed standard injections within the same batch. These two approaches yield exceedingly similar results (Table 4) that were statistically indistinguishable ($p > 0.05$, paired bootstrap). The appeal of this latter approach is that intra-day precision can be routinely calculated without the need for excessive per-sample injections. Regardless of how intra-day precision is quantified, a standard-addition sample to blank-addition sample instrument response ratio of at least 5:1 is suggested to prevent a rapid loss of precision as sample concentration approaches standard addition concentration (Ellison and Thompson, 2008). This feature is shown in Fig. 3 where the precision of a sample is rapidly inflated at high sample concentrations, and we echo the concern that highly concentrated samples require dilution even when technically within the linear range of response. Inter-day precision was assessed across five days for four samples (Table 5) and averaged 12%, although some analytes (e.g., GABA, MurA) showed poorer precision in samples where their concentration was low. Procedural precision, or the variability of replicate extractions of a single sample, was much higher than either intra- or inter-day and averaged 18.7%, although this was quite variable on a per-sample basis (Table 3). Of note, both SRMs had procedural precision much closer to inter-day error, suggesting the possibility that our laboratory's homogenization strategy is inferior to that of the standard reference materials.

Table 4
Intra-day precision calculation method comparison.

Code	Intra-day precision (RSD%)	
	Sample basis	Standard basis
Ala	4.8	6.6
Arg	3.1	5.1
Asp	5.7	6.6
DAPA	8.4	4.6
GABA	7.8	5.0
Glu	6.8	7.6
Gly	6.1	6.3
His	6.1	6.1
Hyp	5.2	5.6
Ile	4.0	5.5
Leu	3.3	6.1
Lys	3.9	4.6
MurA	11.9	6.2
Phe	3.0	5.1
Pro	5.4	6.0
Ser	4.9	5.8
Thr	6.1	6.4
Tyr	4.5	5.1
Val	5.2	6.2

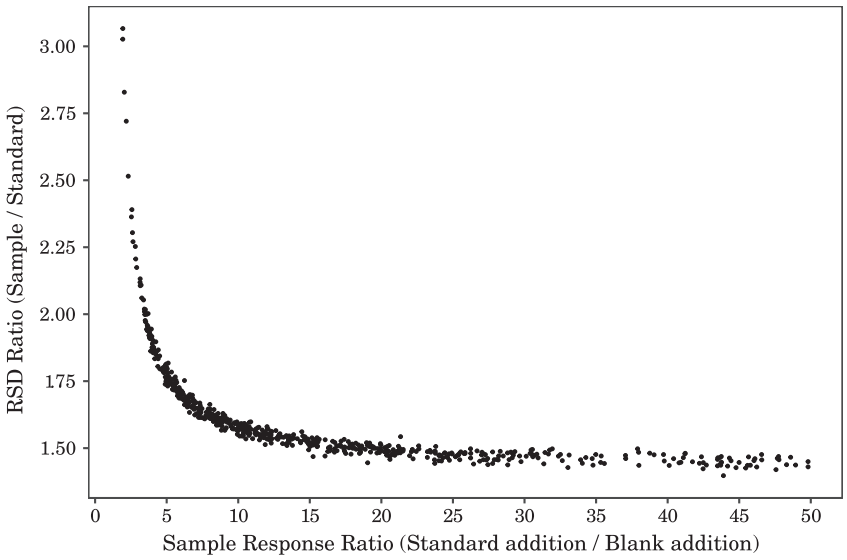

Fig. 3. The effect of standard-addition to blank-addition sample response ratio on instrument precision. Points include all analytes and samples, but the plot is truncated at an X-axis value of 50 to exhibit the asymptotic behavior as the response ratio decreases below 5.

Table 5
Inter-day precision of selected samples.

Code	Inter-day precision (RSD%, $n = 5$)				
	Mean	SRM_1547	SRM_1944	EML_020	EML_183
Ala	12.1	14.1	13.7	9.1	11.5
Arg	12.5	8.2	16.2	11.7	13.9
Asp	13.4	18.1	11.5	11.3	12.5
DAPA	13.5	ND	16.1	12.4	12.0
GABA	14.1	10.4	14.3	21.5	10.0
Glu	13.4	16.9	9.0	14.8	13.1
Gly	11.7	14.0	16.0	8.0	8.8
His	11.8	7.8	14.5	12.2	12.8
Hyp	12.1	12.8	12.8	9.7	13.2
Ile	11.1	10.4	11.4	8.8	14.0
Leu	11.5	10.6	14.5	9.0	12.0
Lys	9.8	5.8	13.9	8.1	11.3
MurA	16.8	ND	12.7	22.6	15.0
Phe	10.9	9.1	12.3	9.6	12.7
Pro	9.9	9.6	9.1	8.9	11.9
Ser	11.0	11.4	10.9	10.1	11.4
Thr	11.4	11.8	13.3	8.8	11.7
Tyr	9.1	7.6	10.7	5.9	12.2
Val	12.2	13.1	13.0	11.3	11.2

ND indicates below detection limit.

3.6. Amino acid composition of natural samples

Total hydrolyzable amino acids (THAA; μmol/g dry sediment) detected here (Table 3 and Supplementary Table S1) were comparable to measurements made by others on soils and plant tissues (Martens and Loeffelmann, 2003; Philben et al., 2014). THAA values were positively correlated with organic carbon contents of soil and sediment samples (Fig. 4a, $r^2 = 0.95$, $p < 0.05$). Secondary amino acids (Hyp, DAPA, GABA) and the amino sugar acid MurA had concentrations that were typically low, but within the range of levels seen in published data (Friedel and Scheller, 2002; Martens and Loeffelmann, 2003; Philben et al., 2014, 2016). We note that our detection of GABA does not explicitly quantify its abundance separately from its isomers α- and β-aminobutyric acid, the latter of which is known to be a naturally occurring plant product and may constitute the apparently high GABA levels in the peach leaf SRM 1547 (Thevenet et al., 2016).

The two bacterially derived compounds DAPA (Gram negative bacteria, West et al., 1987; Philben et al., 2014) and MurA (Gram positive bacteria, Appuhn and Joergensen, 2006; Lomstein and Jorgensen, 2012) were not found in the plant material of SRM 1547, as expected, but were found in all other samples consistent with the accumulation of bacterial residues with soil development. In addition, DAPA and MurA show excellent correlation in this data set (Fig. 4b, $r^2 = 0.94$, $p < 0.05$) suggesting similar patterns of relative contributions from Gram negative and Gram positive bacteria across a wide range of environments (EML – subarctic tundra; WLD – subtropical delta; SRM 1944 – temperate estuarine sediment).

The plant cell wall product Hyp has been postulated to be useful as an indicator of degradation status in peats, where its carbon-normalized concentration increases with oxygen exposure time (Philben et al., 2014). Hyp yields from EML samples are complicated by the long span of time recorded in this data set, as samples at ~100 cm depth have radiocarbon ages reported at ~10,000 yr before present (Hicks Pries et al., 2011). Hyp yields at EML are comparable to Siberian peatlands and their end-members (Philben et al., 2014). While not a peatland, EML shares a high latitude climate setting with the more rapidly accumulating, warmer Siberian peatlands of Philben et al. (2014) with mean annual temperatures just below 0 °C (Hicks Pries et al., 2011). The lack of a downcore trend is consistent with preservation of soil organic matter within permafrost prior to extensive degradation, which Philben and Benner (2013) report is necessary for elevation of Hyp above end-member values. WLD sediments show initially high Hyp yields and do not show obvious trends with depth. The warmer conditions of WLD are likely to allow for much more rapid decomposition of organic matter, and the initially elevated yields may be due to rapid turnover within this system. In place of WLD-specific endmembers, the plant materials used in Philben and Benner (2013) are from a similar setting and are consistent with rapid turnover. Fig. 4c shows a positive, significant relationship of C-normalized Hyp vs DAPA (and MurA, not shown), consistent with the accumulation of microbial products during degradation. However, this relationship appears to be driven by WLD samples and not EML (Fig. 4d), consistent with the former experiencing a higher rate of organic matter turnover, although sample sizes when split by site are small and the regression is non-significant ($p > 0.05$). The peach leaves of SRM 1547 are the only pure plant

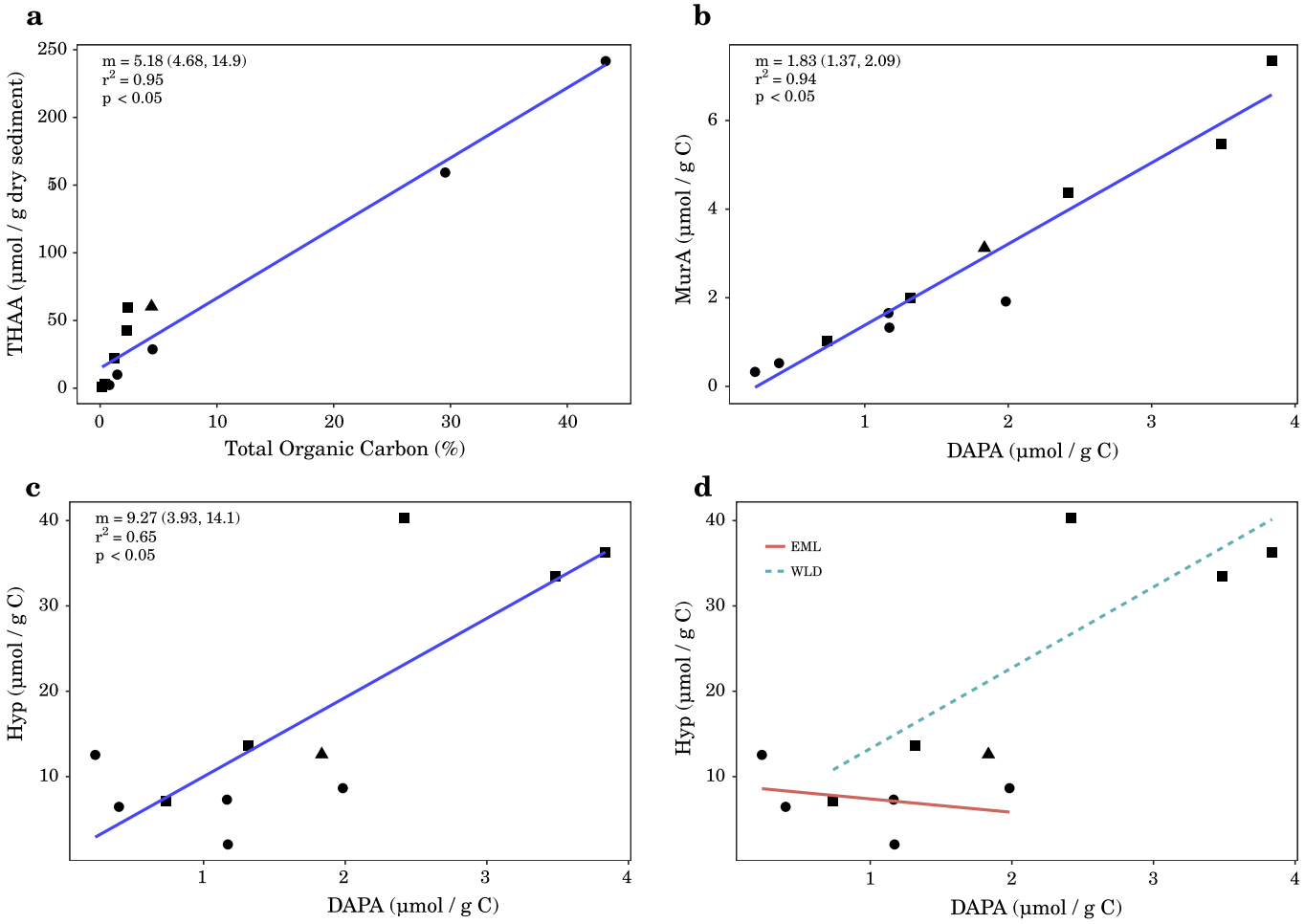

Fig. 4. Scatterplots and associated regressions highlighting the properties of natural samples observed here. Solid circles represent Eight Mile Lake soils, solid squares represent Wax Lake Delta sediments, and the solid triangle represents SRM 1944. No regression summary is shown for (d) due to non-significance.

product measured here and are comparable to higher yields in some crop species reported by Martens and Loeffelmann (2003), but the overall variability of Hyp yields from plants strongly necessitates the use of endmembers when judging the biogeochemical implications of its concentration in natural settings.

3.7. Methodological considerations

This method has several distinct advantages over other published techniques, which are summarized in Table 1. First, sample preparation time is greatly reduced by avoiding solid-phase extraction clean-up, which adds significant time to sample preparation. Published studies listed here all use a strong cation exchange resin that retains amino acids at low pH and elutes at high pH, although similar performance has been observed in other types of exchange columns (Gao et al., 2016). Our testing of this method used self-packed columns, which may have contributed to our poor reproducibility of the de-salting procedure. However, all but one (Roberts and Jones, 2008) of the method papers reviewed here also used self-packed columns. Additionally, explicit extraction reproducibility is only reported by one reference (Amelung and Zhang, 2001) who also report sample-specific recovery issues, although our results with this technique were more extreme. In our experience, the de-salting procedure alone requires approximately a handling time of ~30 min/sample and dilution (used here) requires less than ~3 min/sample when starting with a hydrolyzate. Second, most derivatization procedures are multi-step and necessitate additional sample handling time. We are only familiar with implementing the *o*-phthaldialdehyde method using in-needle automated derivatization, which offers sample handling times competitive with this paper on the order of ~3 min per injection. However, preparation of the *o*-phthaldialdehyde derivatization mixture and the LC mobile phase A buffer can be laborious and should be noted when considering user time investment in an analysis. Third, sample analysis times employed here are superior to practically all other options we have found in the literature. We note that our injection-to-injection time of 9 min is 18 min with a single standard addition. A single injection using the addition of isotopically labeled internal standards could eliminate the need for two injections, but these standards are costly and sometimes difficult to acquire for secondary compounds. Our data suggest that the use of a subset of internal recovery standards would perform poorly at accounting for the widely variable matrix effects seen in natural samples, which is also supported by the recent literature (Liu et al., 2008; Gao et al., 2016). Lastly, our limits of detection are competitive and often superior to alternative methods. We also note that peak integration at low concentrations is, in our experience, more reproducible with MS–MS where there are no nearby peaks within a mass transition compared to photometric detection where the chromatogram is typically only one signal and robust peak-edge detection is difficult near the limit of detection.

4. Conclusions

This paper details a rapid technique for the identification of amino acid concentrations in complex natural matrices. While only hydrolyzable amino acids in soils were explicitly measured here, the instrumental method we detail is applicable to the analysis of amino acids in most natural matrices of interest (e.g., in a dissolved or particulate phase). Our use of a programmable, but still standard issue auto-sampler enables execution of automated standard addition while our chromatographic settings allow for a short analysis. Femtomolar limits of detection enable this method to compete with traditional amino acid techniques while representing reductions in time spent performing sample preparation and analysis. While we only analyzed three naturally occurring secondary amino acids (Hyp, DAPA, GABA) and an amino sugar acid (MurA), the use of MS–MS suggests the instrumental method detailed here is suitable for other, co-extracted secondary compounds as well. The work hours saved using a method that effectively exploits triple quadrupole mass spectrometry is a compelling reason to invest in this technology, but the limitations such as matrix effects are crucial to account for.

Acknowledgments

This work was supported in part by the Jon and Beverly Thompson Chair in Geological Sciences at University of Florida. Alexander Kholodov, Xiaowen Zhang, and Justin Ledman aided in Eight Mile Lake sample collection. Xingqian Cui and Rory Kates aided in Wax Lake Delta sample collection. Kate Dobson aided laboratory preparation of samples. This research did not receive any specific grant from funding agencies in the public, commercial, or not-for-profit sectors. This manuscript was improved by the helpful suggestions of two anonymous reviewers.

Appendix A. Supplementary material

Supplementary data associated with this article can be found, in the online version, at https://doi.org/10.1016/j.orggeochem.2017.10.007.

Associate Editor—**Ann Pearson**

References

Amelung, W., Zhang, X., 2001. Determination of amino acid enantiomers in soils. Soil Biology and Biochemistry 33, 553–562.
Apffel, A., Fischer, S., Goldberg, G., Goodley, P.C., Kuhlmann, F.E., 1995. Enhanced sensitivity for peptide mapping with electrospray liquid chromatography–mass spectrometry in the presence of signal suppression due to trifluoroacetic acid-containing mobile phases. Journal of Chromatography A 712, 177–190.
Appuhn, A., Joergensen, R.G., 2006. Microbial colonisation of roots as a function of plant species. Soil Biology and Biochemistry 38, 1040–1051.
Cowie, G.L., Hedges, J.I., 1994. Biochemical indicators of diagenetic alteration in natural organic matter mixtures. Nature 369, 304–307.
Dauwe, B., Middelburg, J.J., 1998. Amino acids and hexosamines as indicators of organic matter degradation state in North Sea sediments. Limnology and Oceanography 43, 782–798.
Dauwe, B., Middelburg, J.J., Herman, P.M.J., Carlo, H.R.H., 1999. Linking diagenetic alteration of amino acids and bulk organic matter reactivity Abstract—Examination. Limnology and Oceanography 44, 1809–1814.
Davison, A.C., Hinkley, D.V., Schechtman, E., 1986. Efficient bootstrap simulation. Biometrika 73, 555–566.
de Person, M., Chaimbault, P., Elfakir, C., 2008. Analysis of native amino acids by liquid chromatography/electrospray ionization mass spectrometry: comparative study between two sources and interfaces. Journal of Mass Spectrometry 43, 204–215.
Duan, S., Bianchi, T.S., 2007. Particulate and dissolved amino acids in the lower Mississippi and Pearl Rivers (USA). Marine Chemistry 107, 214–229.
Ellison, S.L.R., Thompson, M., 2008. Standard additions: myth and reality. The Analyst 133, 992.
Farrell, M., Hill, P.W., Farrar, J., DeLuca, T.H., Roberts, P., Kielland, K., Dahlgren, R., Murphy, D.V., Hobbs, P.J., Bardgett, R.D., Jones, D.L., 2013. Oligopeptides represent a preferred source of organic N uptake: a global phenomenon? Ecosystems 16, 133–145.
Fountoulakis, M., Lahm, H.-W., 1998. Hydrolysis and amino acid composition analysis of proteins. Journal of Chromatography A 826, 109–134.
Friedel, J.K., Scheller, E., 2002. Composition of hydrolysable amino acids in soil organic matter and soil microbial biomass. Soil Biology & Biochemistry 34, 315–325.
Gao, J., Helmus, R., Cerli, C., Jansen, B., Wang, X., Kalbitz, K., 2016. Robust analysis of underivatized free amino acids in soil by hydrophilic interaction liquid chromatography coupled with electrospray tandem mass spectrometry. Journal of Chromatography A 1449, 78–88.
Harder, U., Koletzko, B., Peissner, W., 2011. Quantification of 22 plasma amino acids combining derivatization and ion-pair LC-MS/MS. Journal of Chromatography B: Analytical Technologies in the Biomedical and Life Sciences 879, 495–504.
Hicks Pries, C.E., Schuur, E.A.G., Crummer, K.G., 2011. Holocene carbon stocks and carbon accumulation rates altered in soils undergoing permafrost thaw. Ecosystems 15, 162–173.
Hobara, S., Osono, T., Hirose, D., Noro, K., Hirota, M., Benner, R., 2014. The roles of microorganisms in litter decomposition and soil formation. Biogeochemistry 118, 471–486.
Hou, S., He, H., Zhang, W., Xie, H., Zhang, X., 2009. Determination of soil amino acids by high performance liquid chromatography-electro spray ionization-mass spectrometry derivatized with 6-aminoquinolyl-N-hydroxysuccinimidyl carbamate. Talanta 80, 440–447.
Huang, Y., Shi, R., Gee, W., Bonderud, R., 2012. Matrix effect and recovery terminology issues in regulated drug bioanalysis. Bioanalysis 4, 271–279.
Jarret, H., Cooksy, K.D., Ellis, B., Anderson, J., 1986. The separation of o-phthalaldehyde derivatives of amino acids by reverse-phase chromatrography on octylsilica columns. Analytical Biochemistry 153, 189–198.
Kaspar, H., Dettmer, K., Chan, Q., Daniels, S., Nimkar, S., Daviglus, M.L., Stamler, J., Elliott, P., Oefner, P.J., 2009. Urinary amino acid analysis: a comparison of iTRAQ®–LC–MS/MS, GC–MS, and amino acid analyzer. Journal of Chromatography B: Analytical Technologies in the Biomedical and Life Sciences 877, 1838–1846.
Konn, C., Magnér, J., Charlou, J.-C., Holm, N.G., Alsberg, T., 2015. A method for detection of trace concentrations of underivatized amino acid in hydrothermal fluids by ion-pairing. American Journal of Analytical Chemistry 6, 313–324.
Kugler, F., Graneis, S., Schreiter, P.P., Stintzing, F.C., Carle, R., 2006. Determination of free amino compounds in betalainic fruits and vegetables by gas chromatography with flame ionization and mass spectrometric detection. Journal of Agricultural and Food Chemistry 54, 4311–4318.
Lindroth, P., Mopper, K., 1979. High performance liquid chromatographic determination of subpicomole amounts of amino acids by precolumn fluorescence derivatization with o-phthaldialdehyde. Analytical Chemistry 51, 1667–1674.
Liu, D.-L., Beegle, L.W., Kanik, I., 2008. Analysis of underivatized amino acids in geological samples using ion-pairing liquid chromatography and electrospray tandem mass spectrometry. Astrobiology 8, 229–241.
Lomstein, B.A., Jorgensen, B.B., 2012. Pre-column liquid chromatographic determination of dipicolinic acid from bacterial endospores. Limnology and Oceanography 10, 227–233.
Martens, D.A., Loeffelmann, K.L., 2003. Soil amino acid composition quantified by acid hydrolysis and anion chromatography–pulsed amperometry. Journal of Agricultural and Food Chemistry 51, 6521–6529.
Matuszewski, B.K., Constanzer, M.L., Chavez-Eng, C.M., 2003. Strategies for the assessment of matrix effect in quantitative bioanalytical methods based on HPLC-MS/MS. Analytical Chemistry 75, 3019–3030.
Menzel, P., Anupama, K., Basavaiah, N., Das, B.K., Gaye, B., Herrmann, N., Prasad, S., 2015. The use of amino acid analyses in (palaeo-) limnological investigations: a comparative study of four Indian lakes in different climate regimes. Geochimica et Cosmochimica Acta 160, 25–37.
Moore, E.K., Harvey, H., Faux, J., Goodlett, D., Nunn, B., 2014a. Electrophoretic extraction and proteomic characterization of proteins buried in marine sediments. Chromatography 1, 176–193.
Moore, E.K., Harvey, H.R., Faux, J.F., Goodlett, D.R., Nunn, B.L., 2014b. Protein recycling in Bering Sea algal incubations. Marine Ecology Progress Series 515, 45–59.
Petritis, K., Chaimbault, P., Elfakir, C., Dreux, M., 2000. Parameter optimization for the analysis of underivatized protein amino acids by liquid chromatography and ionspray tandem mass spectrometry. Journal of Chromatography A 896, 253–263.
Petritis, K., Elfakir, C., Dreux, M., 2002. A comparative study of commercial liquid chromatographic detectors for the analysis of underivatized amino acids. Journal of Chromatography A 961, 9–21.
Petritis, K.N., Chaimbault, P., Elfakir, C., Dreux, M., 1999. Ion-pair reversed-phase liquid chromatography for determination of polar underivatized amino acids using perfluorinated carboxylic acids as ion pairing agent. Journal of Chromatography A 833, 147–155.
Philben, M., Benner, R., 2013. Reactivity of hydroxyproline-rich glycoproteins and their potential as biochemical tracers of plant-derived nitrogen. Organic Geochemistry 57, 11–22.
Philben, M., Kaiser, K., Benner, R., 2014. Does oxygen exposure time control the extent of organic matter decomposition in peatlands? Journal of Geophysical Research: Biogeosciences 119, 897–909.
Philben, M., Ziegler, S.E.S., Edwards, K.K.A., Kahler, R., Benner, R., 2016. Soil organic nitrogen cycling increases with temperature and precipitation along a boreal forest latitudinal transect. Biogeochemistry 127, 397–410.

Piraud, M., Vianey-Saban, C., Petritis, K., Elfakir, C., Steghens, J.-P., Bouchu, D., 2005. Ion-pairing reversed-phase liquid chromatography/electrospray ionization mass spectrometric analysis of 76 underivatized amino acids of biological interest: a new tool for the diagnosis of inherited disorders of amino acid metabolism. Rapid Communications in Mass Spectrometry 19, 1587–1602.

Piraud, M., Vianey-Saban, C., Petritis, K., Elfakir, C., Steghens, J.P., Morla, A., Bouchu, D., 2003. ESI-MS/MS analysis of underivatised amino acids: a new tool for the diagnosis of inherited disorders of amino acid metabolism. Fragmentation study of 79 molecules of biological interest in positive and negative ionisation mode. Rapid Communications in Mass Spectrometry 17, 1297–1311.

Qu, J., Wang, Y., Luo, G., Wu, Z., Yang, C., 2002. Validated quantitation of underivatized amino acids in human blood samples by volatile ion-pair reversed-phase liquid chromatography coupled to isotope dilution tandem mass spectrometry. Analytical Chemistry 74, 2034–2040.

R Core Team, 2017. R: A Language and Environment for Statistical Computing. R Foundation for Statistical Computing, Vienna, Austria. URL http://www.R-project.org/.

Roberts, P., Jones, D.L., 2008. Critical evaluation of methods for determining total protein in soil solution. Soil Biology and Biochemistry 40, 1485–1495.

Rosen, H., 1957. A modified ninhydrin colorimetric analysis for amino acids. Archives of Biochemistry and Biophysics 67, 10–15.

Shields, M.R., Bianchi, T.S., Gélinas, Y., Allison, M.A., Twilley, R.R., 2016. Enhanced terrestrial carbon preservation promoted by reactive iron in deltaic sediments. Geophysical Research Letters 43, 1149–1157.

Thevenet, D., Pastor, V., Baccelli, I., Balmer, A., Vallat, A., Neier, R., Glauser, G., Mauch-Mani, B., 2016. The priming molecule β-aminobutyric acid is naturally present in plants and is induced by stress. New Phytologist. https://doi.org/10.1111/nph.14298.

Tremblay, L., Benner, R., 2006. Microbial contributions to N-immobilization and organic matter preservation in decaying plant detritus. Geochimica et Cosmochimica Acta 70, 133–146.

Trucco, C., Schuur, E.A.G., Natali, S.M., Belshe, E.F., Bracho, R., Vogel, J., 2012. Seven-year trends of CO_2 exchange in a tundra ecosystem affected by long-term permafrost thaw. Journal of Geophysical Research: Biogeosciences 117, Issue G2, CiteID G02031.

Udenfriend, S., Stein, S., Böhlen, P., Dairman, W., Leimgruber, W., Weigele, M., 1972. Fluorescamine: a reagent for assay of amino acids, peptides, proteins, and primary amines in the picomole range. Science 178, 871–872.

Van Hees, P.A.W., Jones, D.L., Finlay, R., Godbold, D.L., Lundström, U.S., 2005. The carbon we do not see – the impact of low molecular weight compounds on carbon dynamics and respiration in forest soils: a review. Soil Biology and Biochemistry 37, 1–13.

Waterval, W.A., Scheijen, J.L., Ortmans-Ploemen, M.M., Habets-van der Poel, C.D., Bierau, J., 2009. Quantitative UPLC-MS/MS analysis of underivatised amino acids in body fluids is a reliable tool for the diagnosis and follow-up of patients with inborn errors of metabolism. Clinica Chimica Acta 407, 36–42.

Werdin-Pfisterer, N.R., Kielland, K., Boone, R.D., 2009. Soil amino acid composition across a boreal forest successional sequence. Soil Biology and Biochemistry 41, 1210–1220.

West, A.W., Grant, W.D., Sparling, G.P., 1987. Use of ergosterol, diaminopimelic acid and glucosamine contents of soils to monitor changes in microbial populations. Soil Biology and Biochemistry 19, 607–612.